Mesocale Convective Systems in Convection Permitting Models under Radiative Convective Equilibrium

Rémy Roca[1],T Fiolleau[1], D Bouniol[2], M Carenso[3], JP Chaboureau[4], G Elsaesser[5,6], B Fildier[3], C Hohenneger[7], C Muller[8] and L Netz[1]

1 Université de Toulouse, Laboratoire d'Etudes en Géophysique et Océanographie Spatiales (CNRS/CNES/IRD/UPS), Toulouse, France ; 2 Centre National de Recherches Météorologiques, CNRS/Météo-France, Toulouse, France ; 3 Laboratoire de Météorologie Dynamique, Institut Pierre Simon Laplace, ENS, Université PSL, Ecole Polytechnique, Institut Polytechnique de Paris, Sorbonne Université, CNRS, Paris, France 4 Laboratoire d'Aérologie (LAERO), Université de Toulouse, CNRS, UT3, IRD, Toulouse, France 5Department of Applied Physics and Mathematics, Columbia University, New York, NY, USA 6 NASA Goddard Institute for Space Studies, New York, NY, USA; 7 Max Planck, Hamburg 8 Institute of Science and Technology Austria ISTA, Klosterneuburg, Austria

Contact information
remy.roca@cnrs.fr

SUMMARY

Organization of deep convection into large upper cloud decks is a fascinating feature of the tropical climate. We analyze radiative convective experiments and km-scale models, following the RCEMIP protocol, and use an object-oriented tracking methodology to explore the link between the system's properties and the bulk climate in RCE. We show that SAM, MESO-NH and ICON-SAPHIRE, despites different bulk features of their equilibrated climate, do share strong similarities at the system life cycle level.

MCS tracking & RCE data

The simulations used here are following the RCEMIP protocol for CRM with a 300K SST (Wing et al., 2018). All integrations are performed as per the original protocol with a specific output frequency of 30min and the use of instantaneous fields instead of hourly averaged. The integration lasts 100 days and the last 25 days only are used and analyzed here to remove spin-up effects (Wing et al., 2020). The 3 model SAM, MNH and ICON are run at a 3km resolution. OLR fields are transformed first in IR brightness temperature (Fig 1a) prior to be segmented using the TOOCAN algorithm (Fig 1b) (Fiolleau and Roca, 2013) to extract the individual MCS from the simulations.

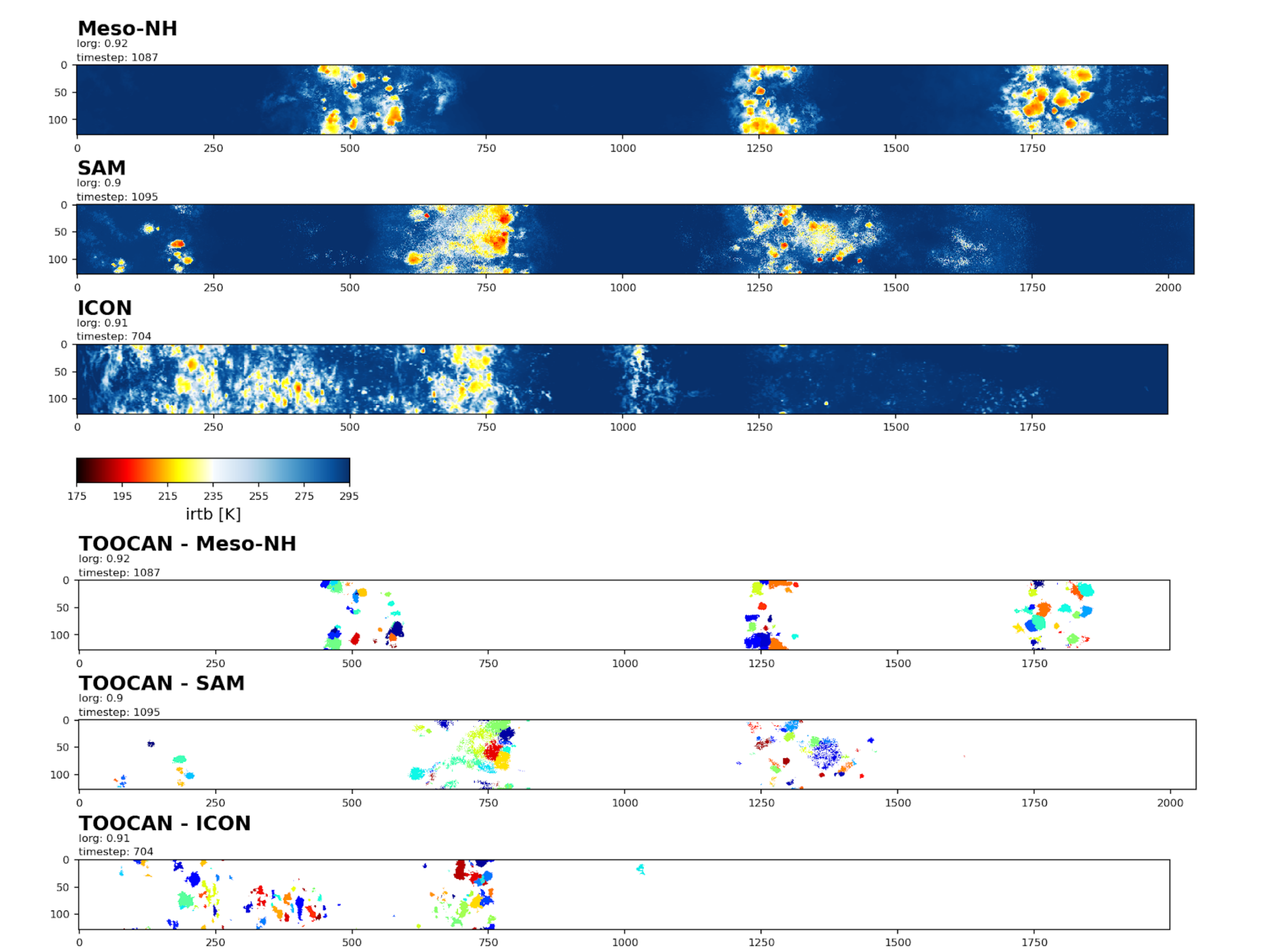

Figure 1 : (top) Snapshot of an instantaneous IRBT (K) field. (Bottom) The TOOCAN segmented results where each color represent an individual MCS

In complement to classic variables, a **convective/stratiform/cirriform mask** is computed from the IR brightness temperature, precipitation and vertical velocity profiles using a simplified implementation of the Physical Threshold Technique proposed in Marinescu et al (2016). A grid box is convective if |w| > 3 m/s below or |w| > 5 m/s above the zero degree isotherm, to account for both updrafts and downdrafts. Furthermore the grid box is set to convective if it rains more than twice its environment or more than 10 mm/h. If not convective and with IRBT<235K and precipitation larger than 0.1 mm/h then it is flagged stratiform and cirriform otherwise.

Bulk RCE state & organization

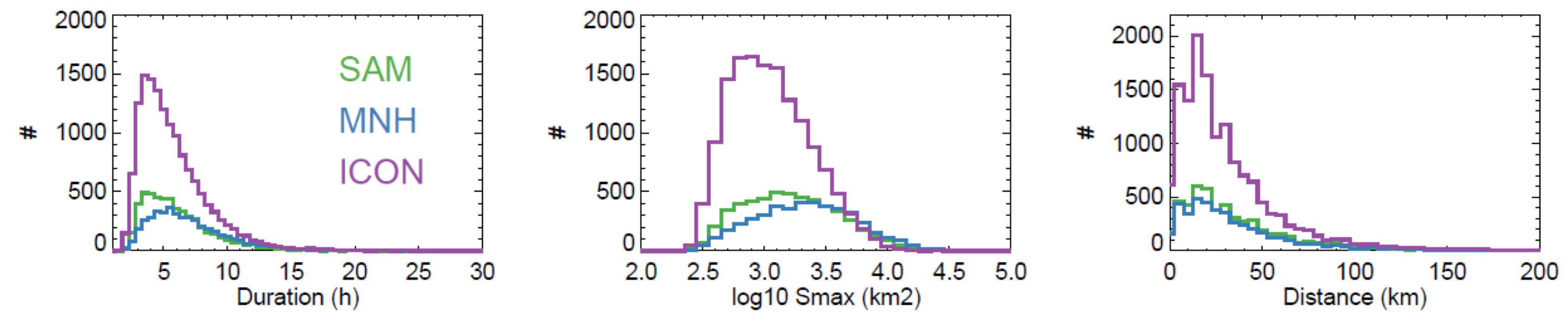

Figure 2 Distribution of individual systems as a function of duration (left), maximum extension (middle) and propagating distance (right) for the 3 models.

	OLR (mean/std) - Wing et al. (2020)		TOOCAN clusters (mean/std))	
Model	COP	Iorg	COP	Iorg
SAM	0.060/0.016	0.86/0.027	0.20/0.07	0.89/0.029
MNH	0.13/0.035	0.91/0.035	0.29/0.08	0.92/0.016
ICON	0.064/0.0098	0.77/0.025	0.11/0.025	0.79/0.033

Table 1 Bulk organization metrics computed for two different definitions of objects : as in Wing et al. (2020) using 4 connected convective pixels or using the TOOCAN clusters.

The simulations show a wide range of convective systems, from short- to long-lived and from small to large, yet **mostly stationary** (Figure 2). ICON exhibits much more systems and is the less organized model according to COP and I_{org} statistics (Table 1).

Life-cycle-resolved morphology

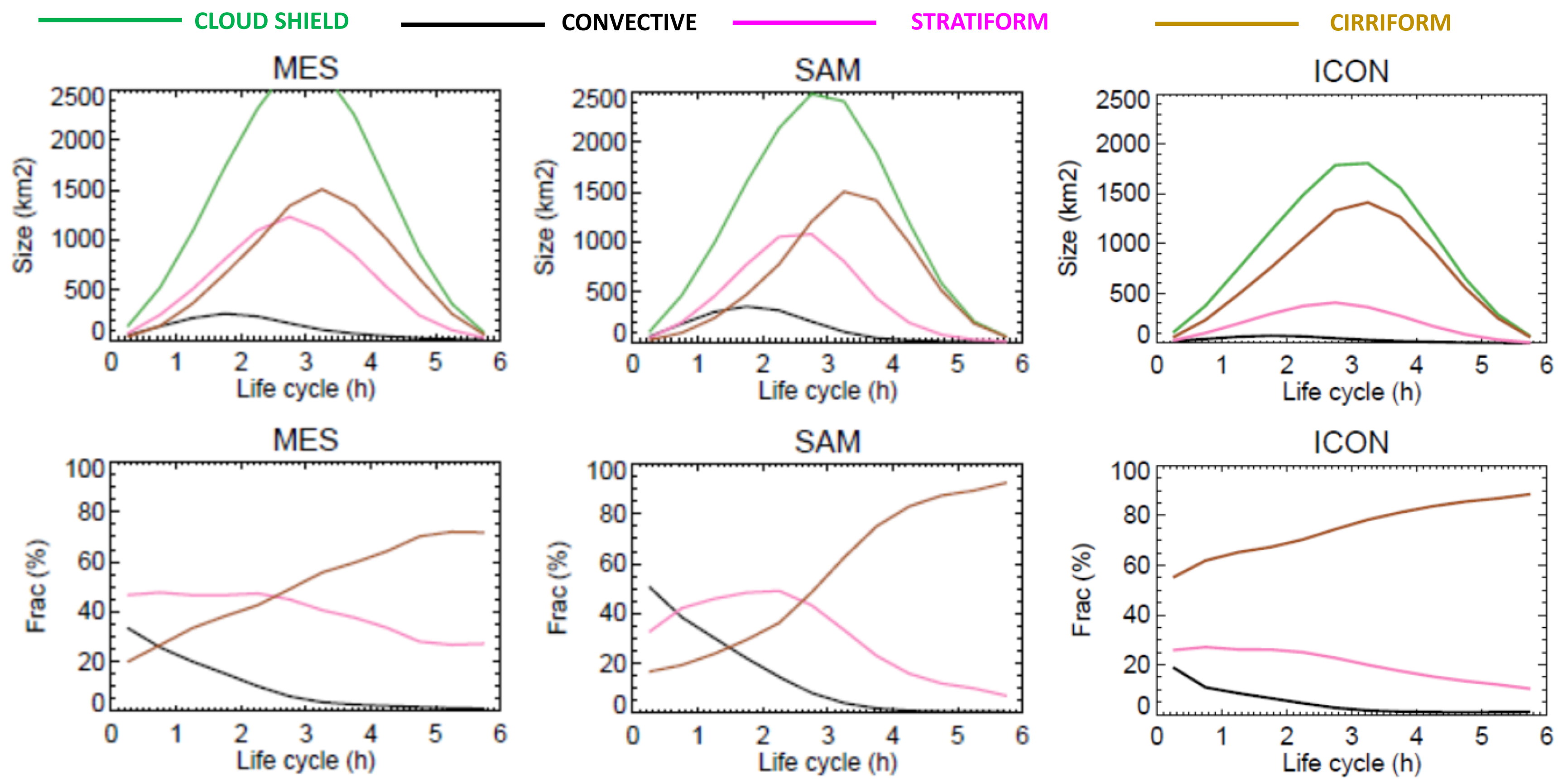

Figure 3 (top) Composite life cycle of the cloud shield area in km2 (green) and the deep convective (black), stratiform (pink) and cirriform (brown) regions (top); (bottom) the relative contribution of each region to the total cloud shield

The life cycle resolved partitioning between convection, stratiform and cirriform parts of the cloud shield follows the generic MCS conceptual model (Houze, 2004) very well for all models. ICON shows less convection and more cirriform fractions.

Life-cycle-resolved heating profile

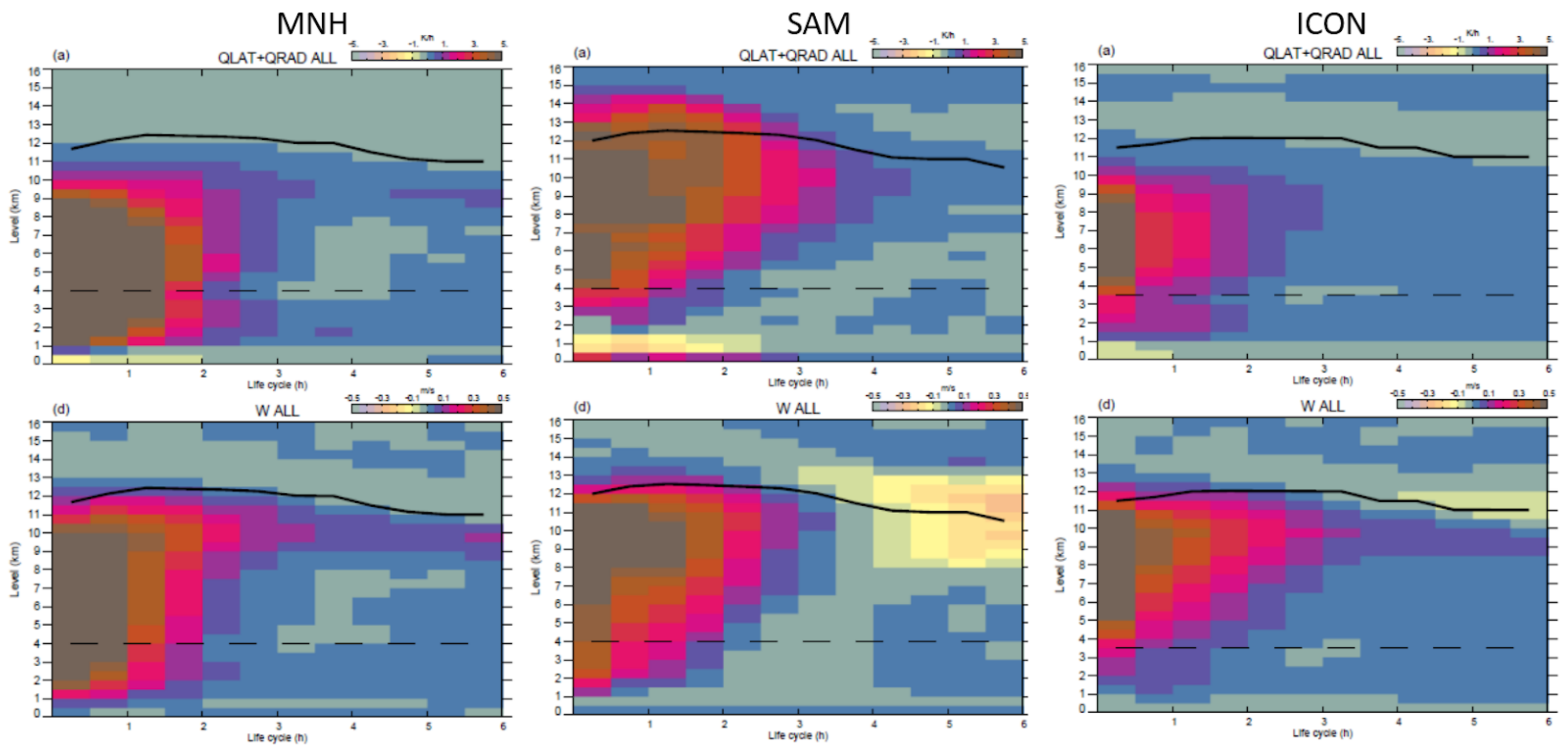

Figure 4 The system-averaged vertical profile of diabatic heating (top) and vertical velocity (bottom) for the 3 models as a function of the life cycle. The black line is the cloud top and the dashed line the melting level.

The system average profile of heating is dominated by latent heat (not shown) and exhibit similarities between the models mainly on the phasing within the life cycle with a **strong mean heating (upward mean motion) mainly in the early part of the system development** but sustained all through the growing phase. Consistent with the disappearance of convection in the decaying phase, the system heating stops at mid life cycle, despites stratiform precipitation. Beyond these robust features, the models deviate from each other in the vertical shape and intensity of the heating and vertical motions with SAM showing more top heaviness than the others. The heating for MNH is deep from the first km up while restricted to the above the melting level for SAM and ICON.

Life-cycle-resolved extreme rain

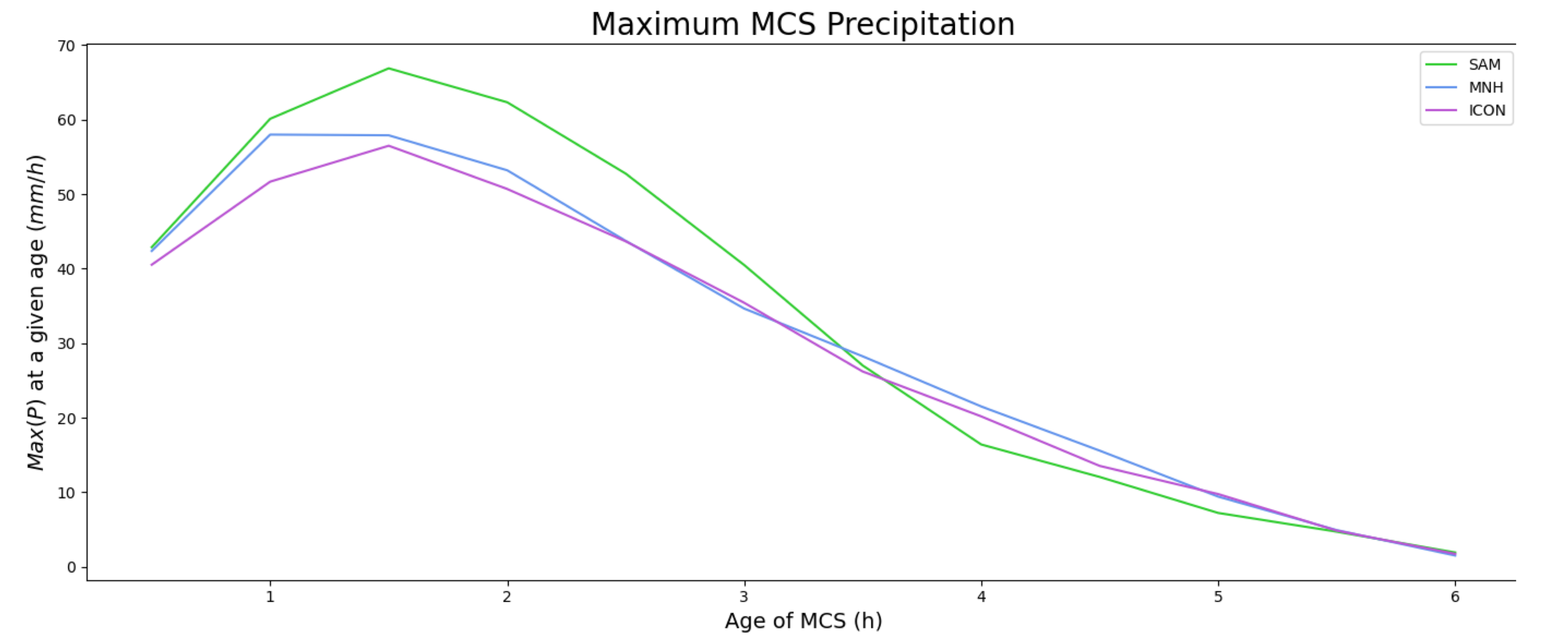

Figure 5 The system maximum grid box level instantaneous rain rate for the 3 models as a function of the life cycle.

Despites difference in the convective dynamic between the models, the phasing and magnitude of the **peak of the system' maximum precipitation at 25% of its life cycle**, in the middle of the shield growing phase, and is robust across the 3 models.

CONCLUSION

Despite drastic differences in their RCE bulk state and distribution of MCS, the individual MCS simulated by the 3 models exhibit **a number of robust and realistic features at the life cycle level**, especially in terms of **phasing of the cold cloud shield and of the precipitation distribution**. These robust features are further reflected in the phasing of the vertical velocity profile life cycle. However, **microphysical differences** among the models are likely the reason for their latent heating profile intensity differences. These morphological resemblances further propagate on the system' extreme precipitation that exhibit a robust magnitude and phasing of its peak at **25% of the life cycle**.

REFERENCES

Houze, R. A., 2004: Mesoscale convective systems. Rev. Geophys., 42, 1–43, https://doi.org/10.1029/2004RG000150 Marinescu, P. J., S. C. van den Heever, S. M. Saleeby, and S. M. Kreidenweis, 2016: The microphysical contributions to and evolution of latent heating profiles in two MC3E MCSs. J. Geophys. Res., 121, 7913–7935, https://doi.org/10.1002/2016JD024762 Fiolleau, T., and R. Roca, 2013: An algorithm for the detection and tracking of tropical mesoscale convective systems using infrared images from geostationary satellite. IEEE Trans. Geosci. Remote Sens., 51, 4302–4315, https://doi.org/10.1109/TGRS.2012.2227762 Wing, A. A., K. A. Reed, M. Satoh, B. Stevens, S. Bony, and T. Ohno, 2018: Radiative-convective equilibrium model intercomparison project. Geosci. Model Dev., 11, 793–813, https://doi.org/10.5194/gmd-11-793-2018 Wing, A. A., and Coauthors, 2020: Clouds and Convective Self-Aggregation in a Multimodel Ensemble of Radiative-Convective Equilibrium Simulations. J. Adv. Model. Earth Syst., 12, 1–38, https://doi.org/10.1029/2020MS002138